

Impact of the top-electrode material on the permittivity of single-crystalline $\text{Ba}_{0.7}\text{Sr}_{0.3}\text{TiO}_3$ thin films

R. Plonka

*Institut für Werkstoffe der Elektrotechnik, RWTH Aachen University of Technology,
D-52056 Aachen, Germany*

R. Dittmann, N. A. Pertsev,^{a)} E. Vasco, and R. Waser

Institut für Festkörperforschung, Forschungszentrum Jülich, D-52425 Jülich, Germany

(Received 18 October 2004; accepted 6 April 2005; published online 13 May 2005)

We observed significant influence of the top-electrode material on the thickness and temperature dependences of the dielectric response of single-crystalline $\text{Ba}_{0.7}\text{Sr}_{0.3}\text{TiO}_3$ thin-film capacitors. For $\text{SrRuO}_3/\text{Ba}_{0.7}\text{Sr}_{0.3}\text{TiO}_3/\text{SrRuO}_3$ samples, the position of dielectric maximum shifts to lower temperatures with decreasing film thickness, whereas the samples with Pt top electrodes exhibit an opposite trend. Moreover, the apparent “interfacial” capacitance, extracted from the film-thickness dependence of dielectric response, is very different for these two types of samples and strongly depends on temperature. Experimental results are analyzed theoretically in light of the depolarizing-field and strain effects on the transition temperature and permittivity of ferroelectric films. © 2005 American Institute of Physics. [DOI: 10.1063/1.1931063]

Collapse of the dielectric response with decreasing thickness, which is observed in perovskite ferroelectric films like $\text{Ba}_x\text{Sr}_{1-x}\text{TiO}_3$ (BST), is an obstacle to the successful integration of these materials as high-permittivity layers in future dynamic random access memories.^{1,2} The collapse is often attributed to the existence of a low-permittivity layer at the film/electrode interface (even though no hint from microstructure investigations exists).^{3,4} In this case, the measured capacitance density c_{eff} can be represented as

$$\frac{1}{c_{\text{eff}}} = \frac{1}{c_{i1}} + \frac{t}{\epsilon_0 \epsilon_b} + \frac{1}{c_{i2}}, \quad (1)$$

where c_{i1} and c_{i2} are the contributions of the supposed interfacial capacitors at two electrodes, and ϵ_b denotes the permittivity of a bulklike film. Besides the presence of a physically distinct low-permittivity layer, some other effects, such as a finite screening length of the electrode,⁵ the soft-mode hardening of surface dipoles,⁶ and the thickness-dependent strain relaxation⁷ also result in a linear thickness dependence of c_{eff}^{-1} similar to Eq. (1).

Several groups reported on a strong influence of the employed electrode material on the dielectric properties of BST films.^{8–10} Izuka *et al.*⁸ found that the room-temperature dielectric response of single-crystalline BST capacitors with Pt top electrode is several times lower than that of capacitors with SRO top electrode. Although this result indicates that oxide electrodes are superior to metallic ones, Pt is one of the most promising materials for the integration of ferroelectrics with complementary metal–oxide–semiconductor technology.

In this letter, we present the dielectric measurements for high-quality single-crystalline BST capacitors with the film thicknesses ranging from 10 to 200 nm. A comparison of capacitors with Pt top electrode (Pt samples) and SRO top electrode (SRO samples), which involve BST layers of the

same crystalline quality, enables us to single out and analyze theoretically the effect of an electrode material on the dielectric response of BST capacitors.

Thin-film capacitors were fabricated on commercial single-crystal (100)-oriented SrTiO_3 (STO) substrates. The SRO/BST bilayers and SRO/BST/SRO trilayers were epitaxially grown *in situ* by pulsed laser deposition (see Ref. 7 for details). The Pt top electrode was *ex situ* deposited on the bilayer samples by dc sputtering. The high-quality cube-on-cube epitaxial relationship between BST, SRO, and STO was proven by x-ray diffraction (XRD) φ -scan measurements ([303]SRO/[303]BST/[303]SRO/[303]STO indexed referring to the pseudocubic SRO unit cell). Rocking curves with a full width of 0.05° at half maximum of the BST (200) peak were measured for both Pt/BST/SRO and SRO/BST/SRO stacks, which indicate that the crystalline quality is independent on the top-electrode material. Furthermore, high-resolution transmission electron microscopy investigations of SRO/BST bilayers and SRO/BST/SRO trilayers proved that no change in the BST microstructure occurs during the deposition of the SRO top electrode.¹¹ The strain state of the BST film at a given thickness t was also found to be the same in both capacitors. This conclusion is based on the thickness dependence of the film's out-of-plane lattice parameter a_3 determined by XRD (see closed symbols in Fig. 1), which fits the same theoretical curve $a_3(t)$ for both SRO and Pt samples. This curve was calculated as described in Ref. 7 under the assumption of thickness-dependent strain relaxation by the formation of misfit dislocations at $t > 10$ nm.

The dielectric measurements were performed with an HP4194 impedance analyzer at 10 kHz and an oscillation voltage level of 100 mV. We measured the capacitance-voltage (C - V) curves of SRO and Pt samples with the BST thickness varying from 10 to 200 nm. For all Pt samples, the maximum of the C - V curve was shifted to $V_{\text{max}} \approx -0.4$ V. This shift can be attributed to an internal electric field caused by different electrode work functions [4.6–4.8 eV for SRO (Ref. 12) and 5.3 eV (Ref. 13) for Pt]. Therefore, we shall

^{a)}Permanent address: A. F. Ioffe Physico-Technical Institute, Russian Academy of Sciences, 194021 St. Petersburg, Russia; electronic mail: pertsev@domain.ioffe.rssi.ru

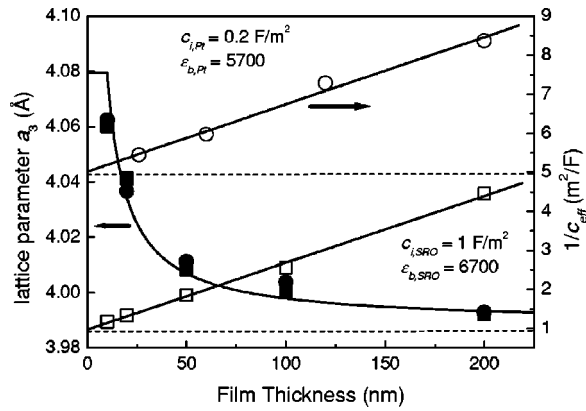


FIG. 1. Thickness dependence of the out-of-plane lattice parameter $a_3(t)$ (closed symbols referred to left vertical axis) and the inverse of the capacitance density (open symbols referred to right vertical axis) for samples with SRO (squares) or Pt (circles) top electrodes at room temperature. The solid curve shows the theoretical dependence $a_3(t)$ (determined in Ref. 7), whereas the straight lines represent linear fits to the experimental data points.

analyze the capacitance values at $V_{\max} = -0.4$ V for Pt samples below.

Variation of the reciprocal capacitance density c_{eff}^{-1} with the film thickness t at room temperature is shown in Fig. 1 by open squares and circles for the SRO and Pt samples, respectively.¹⁴ In agreement with Eq. (1), the data obtained for both types of samples demonstrate a linear thickness dependence with a nonzero intercept, $c_{\text{eff}}^{-1}(t \rightarrow 0) \neq 0$. The slope of this dependence is very similar for both sample series; it corresponds to thick-film permittivities⁷ in the same order of magnitude ($\epsilon_{\infty}^{\text{SRO}} \approx 6700$ versus $\epsilon_{\infty}^{\text{Pt}} \approx 5700$). However, the intercept value was found to be much larger for the Pt samples. Accordingly, the apparent “interfacial” capacitance density in the case of SRO top electrode ($c_i^{\text{SRO}} = 1030$ fF/ μm^2) is about five times higher than the value derived for samples with Pt top electrode ($c_i^{\text{Pt}} = 200$ fF/ μm^2).

Since the thickness dependence of the BST strain state is insensitive to the top-electrode material, the difference between c_i^{SRO} and c_i^{Pt} cannot be attributed to the strain contribution described in Ref. 7. Another contribution results from the reduction of applied electric field inside the film due to a finite screening length of the electrodes.¹⁵ Black and Welser suggested that the interface capacitance density of the SRO electrode is about four times larger than that of the Pt electrode (because the lattice dielectric constant ϵ_m^{SRO} of SRO is expected to be one order of magnitude higher).³ This effect of the electrode material could explain our results for c_i^{SRO} and c_i^{Pt} at room temperature.

We measured capacitances of the Pt and SRO samples in a wide range of temperatures T . Figures 2(a) and 2(b) show the temperature dependences of the apparent dielectric response $\epsilon_{\text{eff}} = c_{\text{eff}} t / \epsilon_0$ obtained for samples with Pt and SRO top electrodes, respectively. Curves 1–3 here correspond to capacitors with three different BST thicknesses. It can be seen that, for all samples, a peak of the dielectric response $\epsilon_{\text{eff}}(T)$ appears at some temperature $T_m(t)$. With decreasing film thickness t , the dielectric peak broadens and its height decreases for both types of capacitors. However, the position $T_m(t)$ of the peak shifts with decreasing film thickness to *higher* temperatures for the Pt samples, whereas for the SRO ones it shifts to *lower* temperatures. Furthermore, the dielec-

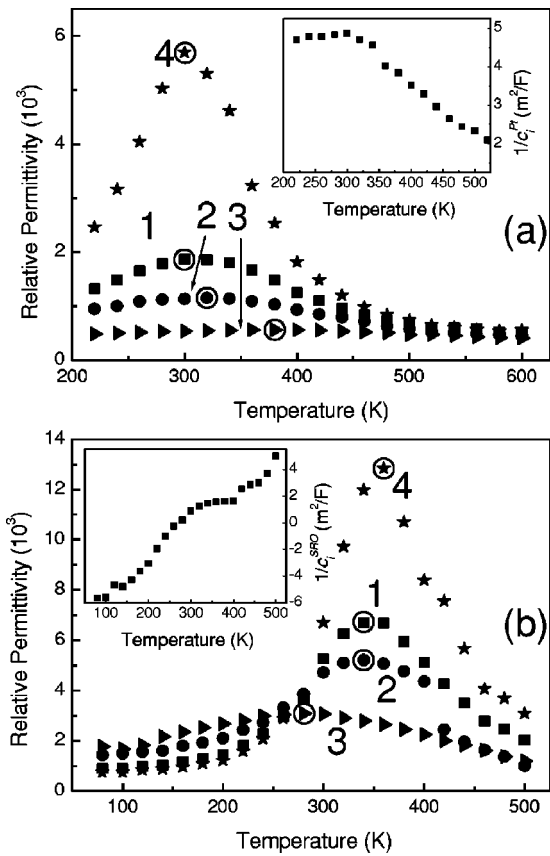


FIG. 2. Temperature dependence of the dielectric response ϵ_{eff} for samples with Pt (a) and SRO (b) top electrodes. Curves (1)–(3) correspond to different BST layer thicknesses: (a) 120 nm (1), 60 nm (2), and 26 nm (3) and (b) 200 nm (1), 100 nm (2), and 50 nm (3). Curve 4 and the insets show the temperature dependences of the thick-film permittivity and the inverse of the interfacial capacitance density (determined from the slope and intercept of the thickness dependence of the reciprocal capacitance, respectively). Circles mark the position of the dielectric maximum for different curves.

tric response ϵ_{eff} of the latter increases with decreasing thickness at temperatures below 260 K [see Fig. 2(b)].

Curves 4 and the insets in Figs. 2(a) and 2(b) show the variations of the thick-film permittivity and the inverse of the interfacial capacitance density, which were extracted from the experimental data using Eq. (1). It should be noted that the maximum thick-film permittivity $\epsilon_{\infty}^{\text{SRO}}(T_m)$ of the SRO samples appears to be more than two times higher than $\epsilon_{\infty}^{\text{Pt}}(T_m)$ of the Pt samples.¹⁶ Moreover, the capacitances c_i^{SRO} and c_i^{Pt} exhibit opposite temperature dependences. Remarkably, the apparent interfacial capacitance c_i^{SRO} of the SRO samples becomes *negative* at low temperatures.

To check whether the above results can be explained by finite screening lengths of the electrodes, we analyzed the properties of ferroelectric capacitors using a simple phenomenological model. In contrast to the previous calculations,⁵ we took into account that the electrode screening ability also affects the temperature T_c of ferroelectric transition, which modifies the thickness dependence of dielectric response additionally. For SRO/BaTiO₃/SRO capacitors, a T_c shift due to incomplete screening of the depolarizing field has been confirmed by first-principles calculations.¹⁷

We modeled the film/electrode interfaces by thin low-permittivity layers with characteristics independent of the film thickness t . Electric fields in the film and the interfacial layers can be evaluated using the continuity condition for the

electric displacement. In the case of a short-circuited capacitor, a depolarizing field $E_{\text{dep}} \equiv -P_3/(c_i t)$ exists inside the film, where P_3 is the film out-of-plane polarization, and c_i is the total interfacial capacitance per unit area. The influence of E_{dep} on the transition temperature T_c can be described with the aid of the nonlinear thermodynamic theory of epitaxial ferroelectric films.¹⁸ The calculation shows that the depolarizing field affects only the second-order polarization term $a_3^* P_3^2$ in the expression for the film thermodynamic potential \tilde{G} derived in Ref. 18. The renormalized coefficient a_3^{**} is given by $a_3^{**} \equiv a_3^* + 1/(2c_i t)$. Since the phase transition in BST films must be of the second order,¹⁸ T_c can be found from the condition $a_3^{**} = 0$, which yields

$$T_c(t) = \theta - \frac{\varepsilon_0 C}{c_i t} + 4 \frac{\varepsilon_0 C Q_{12}}{s_{11} + s_{12}} S_m(t), \quad (2)$$

where θ and C are the Curie–Weiss temperature and constant of the bulk material, s_m are the film elastic compliances, Q_{12} is the electrostrictive constant, and S_m is the misfit strain. Equation (2) shows that the depolarizing-field effect leads to a decrease of T_c in thinner films, which is inversely proportional to the film thickness t and to the capacitance c_i . Similar thickness dependence is displayed by the temperature T_m of the dielectric maximum in our SRO samples and in Pt/BST/Pt and $\text{La}_{0.5}\text{Sr}_{0.5}\text{CoO}_3/\text{BST}/\text{Au}$ capacitors studied in Refs. 19 and 20. At the same time, the misfit-strain effect, described by the last term in Eq. (2), leads to an increase in the transition temperature T_c with decreasing thickness in our case of BST films grown on SRO/STO, because S_m is negative here and its magnitude increases in thinner films.⁷ This trend is similar to the thickness dependence of the dielectric-peak position T_m observed in our Pt samples and in SRO/BST/Au capacitors investigated in Ref. 21.

To calculate the out-of-plane permittivity ε_{33} of an epitaxial BST film, we may use the P^4 approximation. If only the out-of-plane polarization P_3 differs from zero (we have $S_m < 0$), $\varepsilon_{33} \equiv (2a_3^{**} + 12a_{33}^* P_3^2)^{-1}$, where a_{33}^* is the renormalized fourth-order coefficient.¹⁸ At $T > T_c(t)$, when the film is in the paraelectric state, $P_3 = 0$ and $\varepsilon_{33} \equiv (2a_3^{**})^{-1}$. Taking into account the presence of an interfacial capacitance c_i during the dielectric measurements, for the sample capacitance we obtain the relation $c_{\text{eff}}^{-1} \equiv t/\varepsilon_{33}^0(P_3=0) + 2/c_i$, where ε_{33}^0 is the film permittivity in the absence of the depolarizing-field effect ($1/c_i \rightarrow 0$). Below the transition temperature $T_c(t)$, $P_3^2 = -a_3^{**}/[2a_{33}^*]$ so that $\varepsilon_{33} \equiv -(4a_3^{**})^{-1}$ and

$$\frac{1}{c_{\text{eff}}} \equiv \frac{t}{\varepsilon_{33}^0(P_3 \neq 0)} - \frac{1}{c_i}. \quad (3)$$

Equation (3) demonstrates that the thickness dependence of the reciprocal capacitance c_{eff}^{-1} can have a *negative* intercept. This unexpected theoretical result may explain the observed behavior of SRO/BST/SRO capacitors at low temperatures [Fig. 2(b) inset]. At sufficiently high temperatures, where all films in the studied thickness range of $t_{\text{min}} \leq t \leq t_{\text{max}}$ are in the paraelectric state, the intercept must be positive, which also agrees with our data for SRO samples.

Unfortunately, Eqs. (2) and (3) cannot explain the observed behavior of Pt/BST/SRO capacitors. Indeed, since the interface capacitance density of the Pt electrode is expected to be smaller than that of the SRO one,⁵ the depolarizing-field effect should be even stronger in the Pt samples, pre-

vailing over the misfit-strain effect as well. Accordingly, Eq. (2) predicts the dielectric-peak shift to lower temperatures with decreasing film thickness, which is inconsistent with the data shown in Fig. 2(a). On the other hand, the presence of two different electrodes in the Pt samples could lead to an increase of T_m in thinner films.²² This explanation may be valid, however, only if the internal electric field is not completely compensated by the applied field in our experiments.

Since the influence of electrode material on the film permittivity is likely to result from a superposition of several different effects, the dielectric behavior of SRO/BST/SRO and Pt/BST/SRO capacitors cannot be consistently described by our model in a wide temperature range. Nevertheless, one of the most remarkable experimental results, namely, the increase of dielectric response with decreasing thickness observed for SRO/BST/SRO samples at low temperatures, can be explained by the decrease of ferroelectric transition temperature due to the depolarizing-field effect.

The research described in this publication was made possible, in part, by Grant No. I/75965 from the Volkswagen-Stiftung, Germany.

¹D. E. Kotecki, J. D. Baniecki, H. Shen, R. B. Laibowitz, K. L. Saenger, J. J. Lian, T. M. Shaw, S. D. Athavale, C. Cabral, Jr., P. R. Duncombe, M. Gutsche, G. Kunkel, Y.-J. Park, Y.-Y. Wang, and R. Wise, IBM J. Res. Dev. **43**, 151 (2000).

²N. Setter and R. Waser, Acta Mater. **48**, 151 (2000).

³S. K. Streiffer, C. Basceri, C. B. Parker, S. E. Lash, and A. Kingon, J. Appl. Phys. **86**, 4565 (1999).

⁴L. J. Sinnamon, R. M. Bowman, and J. M. Gregg, Appl. Phys. Lett. **78**, 1724 (2001).

⁵C. T. Black and J. J. Welser, IEEE Trans. Electron Devices **46**, 776 (1999).

⁶C. Zhou and D. M. Newns, J. Appl. Phys. **82**, 3081 (1997).

⁷R. Dittmann, R. Plonka, E. Vasco, N. A. Pertsev, J. Q. He, C. L. Jia, S. Hoffmann-Eifert, and R. Waser, Appl. Phys. Lett. **83**, 5011 (2003).

⁸M. Izuka, K. Abe, and N. Fukushima, Jpn. J. Appl. Phys., Part 1 **36**, 5866 (1997).

⁹Y. A. Boikov and T. Claeson, Appl. Phys. Lett. **80**, 4603 (2002).

¹⁰C. S. Hwang, J. Appl. Phys. **92**, 432 (2002).

¹¹J. Q. He, E. Vasco, C. L. Jia, R. Dittmann, and R. H. Wang (unpublished).

¹²A. J. Hartmann, M. Neilson, R. N. Lamb, K. Watanabe, and J. F. Scott, Appl. Phys. A: Mater. Sci. Process. **70**, 239 (2000).

¹³J. F. Scott, *Ferroelectric Memories* (Springer, Berlin, 2000).

¹⁴The data for capacitance densities c_{eff} represent average values for capacitors of three different areas A (10 000, 2500, and 900 μm^2). No size dependence $c_{\text{eff}}(A)$ was observed.

¹⁵H. Y. Ku and F. G. Ullman, J. Appl. Phys. **35**, 265 (1964).

¹⁶Our experimental data also show that the strong suppression of the film dielectric peak, which was postulated recently by A. M. Bratkovski and A. P. Levanyuk (cond-mat/0410263) for asymmetric capacitors, is absent in high-quality ferroelectric films. Indeed, their phenomenological model predicts that, owing to a surface bias field, the maximum permittivity of BST films decreases down to $\varepsilon(T_m) < 1000$ already at $t \sim 1000$ nm. In contrast, the measured dielectric response $\varepsilon(T_m)$ of our asymmetric Pt/BST/SRO capacitors remains to be about 2000 even at $t = 120$ nm.

¹⁷J. Junquera and P. Ghosez, Nature (London) **422**, 506 (2003).

¹⁸N. A. Pertsev, A. G. Zembilgotov, and A. K. Tagantsev, Appl. Phys. Lett. **80**, 1988 (1998); Ferroelectrics **223**, 79 (1999).

¹⁹C. B. Parker, J.-P. Maria, and A. I. Kingon, Appl. Phys. Lett. **81**, 340 (2002).

²⁰A. Lookman, R. M. Bowman, J. M. Gregg, J. Kut, M. Dawber, A. Rue-diger, and J. F. Scott, J. Appl. Phys. **96**, 555 (2004).

²¹L. J. Sinnamon, R. M. Bowman, and J. M. Gregg, Appl. Phys. Lett. **81**, 889 (2002).

²²W. J. Merz, Phys. Rev. **91**, 513 (1953); H.-M. Christen, J. Mannhart, E. J. Williams, and C. Gerber, Phys. Rev. B **49**, 12095 (1994); Y. A. Boikov and T. Claeson, Phys. Solid State **43**, 2267 (2001).